ADVANCES IN
CIVIL ENGINEERING

Proceedings of the 1st
Conference on Advances in Civil Engineering (ICACE 2022) Vinh University, Vietnam

Website: http://www.nxbkhkt.com
Hotline: 0898 275 999
Email: nxbkhkt@hn.vnn.vn

222230B00
ISBN 9786046724100
9 786046 724100

Assoc.Prof Tran Ngoc Long
Dr. Nguyen Trong Ha
Dr. Nguyen Duy Duan

ADVANCES IN CIVIL ENGINEERING

VINH UNIVERSITY, VIETNAM

Editors:
Assoc.Prof Tran Ngoc Long
Dr. Nguyen Trong Ha
Dr. Nguyen Duy Duan

ADVANCES IN CIVIL ENGINEERING

Proceedings of the 1st

Conference on Advances in Civil Engineering (ICACE 2022)
Vinh University, Vietnam

Vinh University, Vietnam

SCIENCE AND TECHNICS PUBLISHING HOUSE

Editors:

Assoc. Prof. Tran Ngoc Long

Dr. Nguyen Trong Ha - Dr. Nguyen Duy Duan

ADVANCES IN CIVIL ENGINEERING

Proceedings of the 1st Conference on Advances in Civil Engineering (ICACE 2022)

Vinh University, Vietnam

SCIENCE AND TECHNICS PUBLISHING HOUSE

Hanoi - 2022

ICACE-2022 Scientific Committee

Chairs

Prof. TRAN Minh Tu, Hanoi University Civil Engineering, Vietnam

Prof. TRAN The Truyen, University of Transport and Communications, Vietnam

Members

Prof. LEE Tae-Hyung, Konkuk University, Korea

Prof. BUI Quoc Tinh, Tokyo Institute of Technology, Japan

Prof. HA Dong-Ho, Konkuk University, Korea

Prof. PARK Duhee, Hanyang University, Korea

Prof. THAI Huu Tai, The University of Melbourne, Australia

Prof. LY Quang Viet, Tianjin Polytechnic University, China

Prof. KIM Seung-Eock, Sejong University, Korea

Dr. CHANA Sinsabvarodom, NTNU, Norway

Dr. DO Trong Nhan, National Cheng Kung University, Taiwan

Dr. GAUTAM Dipendra, Interdisciplinary Research Institute for Sustainability (IRIS), Nepal

Prof. SADIQ Shamsher, Ghulam Ishaq Khan Institute of Engineering Sciences and Technology, Pakistan

Prof. HO Huu Loc, Asian Institute of Technology, Thailand

Prof. NGUYEN Ngoc Tan, Sejong University, Korea

Prof. TRINH Minh Chien, Chonbuk National University, Korea

Dr. HO Sy Lanh, Hiroshima University, Japan

Dr. NGUYEN Van Dong, Chonnam National University, Korea

Dr. NGUYEN Duc Hai, Sejong University, Korea

Dr. PHAM Luong, RMIT University, Australia

Prof. LE Thang, California State University, Northridge, USA

Dr. TRAN Vinh Loc, Ton Duc Thang University, Vietnam

Dr. PHAM Thai Hoan, National University Civil Engineering, Vietnam

Dr. NGUYEN Van Quang, Vinh University, Vietnam

Dr. TRAN Viet Linh, Vinh University, Vietnam

ICACE-2022 Organizing Committee

Chairs

Prof. NGUYEN Huy Bang, Vinh University, Vietnam (Chair)

Dr. TRAN Ba Tien, Vinh University, Vietnam (Co-Chair)

Dr. TRAN Ngoc Long, Vinh University, Vietnam (Co-Chair)

Members

Assoc. Prof. MAI Van Chung, Vinh University, Vietnam

Mr. NGUYEN Hong Soa, Vinh University, Vietnam

Mr. HOANG Viet Dung, Vinh University, Vietnam

Mr. NGUYEN Van Hai, Vinh University, Vietnam

Prof. DINH Xuan Khoa, Vinh University, Vietnam

Dr. PHAN Van Tien, Vinh University, Vietnam

Dr. LE Thanh Hai, Vinh University, Vietnam

Dr. PHAM Hong Son, Vinh University, Vietnam

Dr. PHAN Van Phuc, Vinh University, Vietnam

Dr. NGUYEN Trong Kien, Vinh University, Vietnam

Secretariats

Dr. NGUYEN Trong Ha, Vinh University, Vietnam

Dr. NGUYEN Duy Duan, Vinh University, Vietnam

Mr. TRAN Xuan Vinh, Vinh University, Vietnam

Mr. NGUYEN Tien Hong, Vinh University, Vietnam

Mr. NGUYEN Duy Khanh, Vinh University, Vietnam

Mr. NGUYEN Manh Hung, Vinh University, Vietnam

PREFACE

On the occasion of celebrating the 20-year anniversary of the Department of Civil Engineering, Vinh University, the International Conference on Advances in Civil Engineering (ICACE-2022) was organized to connect the faculties of the Department of Civil Engineering research professionals, scholars, and scientists from different institutions both in Vietnam and abroad. ICACE-2022 was organized on May 21st, 2022, at Vinh University, Vietnam. This event was a good opportunity to discuss new research findings in the civil engineering field. We believe that those updated studies will contribute to solving the practical problems. The main topics of the conference included Structural and mechanics engineering, Construction and building materials, Smart and sustainable infrastructure, Geotechnical engineering, Hydraulic, pavement, costal and offshore engineering, and Construction engineering and project management. This proceeding includes the full papers selected from the accepted submissions, which were presented at ICACE-2022.

On behalf of the Organizing Committee, we are sincerely thankful for the contribution of two keynote lectures, which are presented by Prof. Tran Minh Tu (Hanoi University of Civil Engineering, Vietnam) and Assoc. Prof. Tran The Truyen (University of Transportation and Communication, Vietnam). Additionally, a great appreciation is to all authors who submitted papers and presented at the parallel sessions. We also want to give our sincere thanks to companies and Vinh University for their support. Their contributions made the conference a success.

Assoc. Prof. Tran Ngoc Long

On behalf of the Organizing Committee of ICACE-2022

Dean of Department of Civil Engineering, Vinh University

CONTENTS

Vibration analysis of functionally graded porous plates resting on Kerr elastic foundations

Van-Long Nguyen [1], Minh-Tu Tran [1], Thanh-Hai Le [2], Xuan-Thuc Phan[2]*

[1] Ha Noi University of Civil Engineering, 55 Giai Phong Road, Hanoi, Viet Nam
[2] Vinh University, 182 Le Duan Road, Vinh, Nghe An, Viet Nam

**Email: longnv@huce.edu.vn*

Abstract. This paper presents the free vibration analysis of functionally graded porous materials (FGPMs) plates, in the framework of classical plate theory (CPT). The plate is rested on Keer's elastic foundation with the three-parameter elastic model. Functional graded porous material, in particular, open-cell metal foam with porosities that vary smoothly along thickness direction according to three porosity distribution patterns: uniform, nonuniform symmetric and nonuniform asymmetric are considered. Based on Hamilton's principle, the equations of motion are derived. The numerical examples are performed and compared with those available in the literature to show the accuracy of the present results. The effect of porosity coefficient, porosity distribution patterns, geometrical and Kerr elastic foundation parameters on natural frequencies are investigated.

Keywords: Vibration analysis, functionally graded porous plate, classical plate theory, Kerr elastic foundations.

1. Introduction

Functionally graded porous materials (FGPMs) are a new class of functionally graded materials that in the microstructure there are internal pores with local density and size distributed according to certain rules, so the material properties can be considered as smoothly and continuously changing in the space of structures. Metal foam is one of the highly porous materials with cellular structures possessing many outstanding properties, such as excellent energy-absorbing capability, electrical conductivity, and thermal management, thus they are widely used in aerospace engineering, automotive industry, and civil constructions. An in-depth understanding of the mechanical behaviors of FGP structures is pivotal in the design, construction and maintenance process.

Vibration is one of the important problems in the design of structural elements, thus a study of their vibrational characteristics attracted the local and international scientific community. Chen et al. [1] investigated the effect of porosity distribution patterns and porosity coefficient on free and forced vibration characteristics of FGP beams. Employing the differential transformation method, Wattanasakulpong et al [2] presented the linear and nonlinear analysis of FG beams under different types of elastic supports. Leclaire [3] analyzed the free vibrations of a rectangular thin FGP plate with liquid. Using three-dimensional elastic theory, Zhao et al. [4] studied the free vibration of thick rectangular FGP plates with various boundary conditions. Zhao et al. used an improved Fourier series method to analyze the free vibration of the Mindlin porous plate [5]. Using the state space approach and a four-variable plate theory, Demirhan et al. [6] investigated the free vibration and bending behavior of FGP plate with two opposite simply-supported edges. Tran et al. [7] analyzed the static and free vibration of FGP variable-thickness plates by employing an edge-based smoothed finite element method (ES-FEM).

The interaction action between structures and elastic foundations is an important topic and always attracted the attention of designers. Arani et al [8] studied the free vibration of an FGP rectangular plate resting on a Winkler foundation using Reddy's third-order shear deformation theory and differential quadrature method. Hashemi et al. [9] non-linear free vibration analysis of a bidirectional functional hierarchical rectangular plate in a plane with voids located on a Winkler-Pasternak elastic foundation. Based on the sinusoidal shear deformation theory and analytical approach, Benferhat et al. [10] investigated the effect of porosity on bending and free vibration behavior of simply supported FGP plate resting on the Winkler-Pasternak foundation. Zaoui et al. presented a closed-form solution to predict the fundamental natural frequency of FG plate substrates on Pasternak elastic foundation by using two dimensional (2D) and quasi three dimensional (quasi-3D) shear deformation theories. Huang et al. [11] nonlinear free and forced vibrations of FGP plates on nonlinear elastic foundations. Shahsavari et al. [12] used a novel quasi-3D hyperbolic theory is presented for the free vibration analysis of functionally graded (FGP) porous plates resting on elastic foundations with a Winkler/Pasternak/Kerr foundation (three-parameter elastic model). Utilizing the Navier solution technique, Kim et al. [13] investigated the bending, free vibration, and buckling response of FGP micro-plates resting on Winkler/Pasternak/Kerr elastic foundation using the classical and first-order shear deformation plate theories. Kerr's elastic foundation model was also used in the study on free vibration of simply supported FG sandwich plates of Daikh [14].

In this paper, the basic relationships and governing equations are established to analyze the free vibration of the FGP plates resting on Kerr's elastic foundation in the framework of the classical plate theory. Uniform, nonuniform symmetric and nonuniform asymmetric porosity distribution patterns of FGPM are considered. Navier's technique is used to determine the natural frequency of the simply supported rectangular FGP plate. Verification examples are performed through comparison with some existing results. The effect of porosity coefficient, porosity distribution patterns, Kerr elastic foundation parameters and geometrical parameters on natural frequencies is investigated in detail.

2. Theoretical formulation

2.1. The functionally graded porous plate

Consider a thin rectangular FGP plate of length *a*, width *b* and thickness *h*, respectively as shown in Fig. 1, referring to the rectangular Cartesian coordinates (*x, y, z*), where (*x, y*) plane coincides with the middle surface of the plate and *z* is the thickness coordinate ($-h/2 \le z \le h/2$). The plate is rested on Keer's elastic foundation with a three-parameter elastic model including an independent upper (with stiffness K_u), shear (with stiffness K_s) and lower (with stiffness K_l) elastic layers.

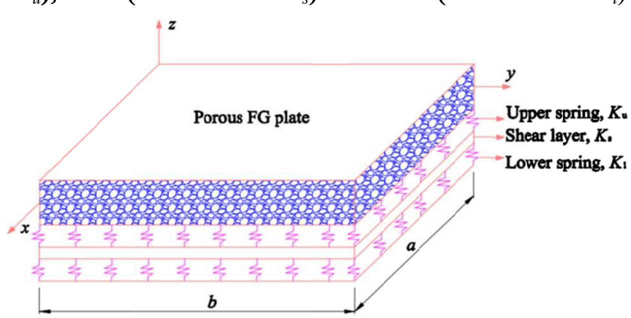

Fig. 1. The configuration of rectangular FGP plates resting on the Kerr foundation.

Three different porosity distribution patterns are considered as follows [1, 15, 16]:

- Uniform porosity distribution (Type 1- Fig. 2-a):

$$\begin{aligned}&\{E,G\}=\{E_{\max},G_{\max}\}(1-e_0\lambda);\\&\rho=\rho_{\max}\sqrt{1-e_0\lambda};\\&\lambda=\frac{1}{e_0}-\frac{1}{e_0}\left(\frac{2}{\pi}\sqrt{1-e_0}-\frac{2}{\pi}+1\right)^2.\end{aligned} \tag{1}$$

- Non-uniform symmetric distribution (Type 2- Fig. 2-b):

$$\{E(z),G(z)\}=\{E_{\max},G_{\max}\}\left[1-e_0\cos\left(\frac{\pi z}{h}\right)\right];$$
$$\rho(z)=\rho_{\max}\left[1-e_m\cos\left(\frac{\pi z}{h}\right)\right]. \tag{2}$$

- Non-uniform asymmetric distribution (Type 3- Fig. 2-c):

$$\{E(z),G(z)\}=\{E_{\max},G_{\max}\}\left[1-e_0\cos\left(\frac{\pi z}{2h}+\frac{\pi}{4}\right)\right];$$
$$\rho(z)=\rho_{\max}\left[1-e_m\cos\left(\frac{\pi z}{2h}+\frac{\pi}{4}\right)\right]. \tag{3}$$

where $E_{\max}$, $G_{\max}$, and $\rho_{\max}$ are the maximum values of elasticity moduli, shear moduli and mass density; $E_{\min}$, $G_{\min}$, and $\rho_{\min}$ denote the minimum values, respectively. The porosity coefficients are defined by:

$$e_0=1-\frac{E_{\min}}{E_{\max}}=1-\frac{G_{\min}}{G_{\max}}\ (0<e_0<1);$$
$$e_m=1-\frac{\rho_{\min}}{\rho_{\max}}=1-\sqrt{1-e_0}\quad(0<e_m<1). \tag{4}$$

Poisson's coefficient v is assumed to be constant along with the plate thickness.

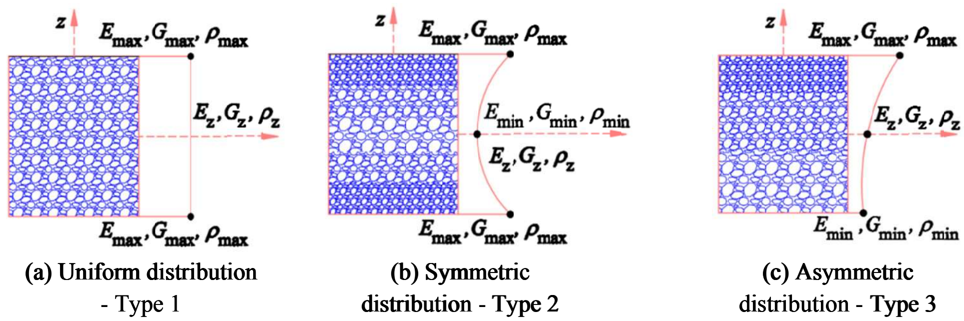

Fig. 2. The FGP plate with different porosity density distribution patterns.

2.2. Classical plate theory (CPT) - Equations of motion

Based on CPT, the displacement components (u, v, w) along x, y and z axes of an arbitrary point (x, y, z) of the FGP plate are expressed as follows [17]:

$$u(x,y,z,t)=u_0(x,y,t)-zw_{0,x};\ v(x,y,z,t)=v_0(x,y,t)-zw_{0,y};$$
$$w(x,y,z,t)=w_0(x,y,t). \tag{5}$$

in which: t is a time variable; u_0, v_0, w_0 are the displacement components in the mid-plane.

The strain components based on the CPT can be written as follows [17]:

$$\begin{Bmatrix}\varepsilon_x\\ \varepsilon_y\\ \gamma_{xy}\end{Bmatrix}=\begin{Bmatrix}\varepsilon_x^0\\ \varepsilon_y^0\\ \gamma_{xy}^0\end{Bmatrix}+z_{ns}\begin{Bmatrix}\kappa_x\\ \kappa_y\\ \kappa_{xy}\end{Bmatrix} \tag{6}$$

where: $\varepsilon_x^0 = u_{0,x}$; $\varepsilon_y^0 = v_{0,y}$; $\gamma_{xy}^0 = u_{0,y} + v_{0,x}$; $\kappa_x = -w_{0,xx}$; $\kappa_y = w_{0,yy}$; $\kappa_{xy} = -2w_{0,xy}$.

The commas subscripts denote the partial differentiation with respect to the spatial variables Stresses are determined from Hooke's law and written as:

$$\begin{Bmatrix} \sigma_x \\ \sigma_y \\ \sigma_{xy} \end{Bmatrix} = \begin{bmatrix} Q_{11} & Q_{12} & 0 \\ Q_{21} & Q_{22} & 0 \\ 0 & 0 & Q_{66} \end{bmatrix} \begin{Bmatrix} \varepsilon_x \\ \varepsilon_y \\ \gamma_{xy} \end{Bmatrix} \tag{7}$$

in which: $Q_{11} = Q_{22} = \dfrac{E(z)}{1-\nu^2}$; $Q_{12} = Q_{21} = \dfrac{\nu E(z)}{1-\nu^2}$; $Q_{66} = \dfrac{E(z)}{2(1+\nu)}$.

The force and moment resultants per unit length of the plate are defined as:

$$\begin{Bmatrix} N_x \\ N_y \\ N_{xy} \end{Bmatrix} = \begin{bmatrix} A_{11} & A_{12} & 0 \\ A_{12} & A_{11} & 0 \\ 0 & 0 & A_{66} \end{bmatrix} \begin{Bmatrix} \varepsilon_x^0 \\ \varepsilon_y^0 \\ \gamma_{xy}^0 \end{Bmatrix}; \begin{Bmatrix} M_x \\ M_y \\ M_{xy} \end{Bmatrix} = \begin{bmatrix} D_{11} & D_{12} & 0 \\ D_{12} & D_{11} & 0 \\ 0 & 0 & D_{66} \end{bmatrix} \begin{Bmatrix} \kappa_x \\ \kappa_y \\ \kappa_{xy} \end{Bmatrix} \tag{8}$$

where: $A_{11} = \dfrac{E_1}{1-\nu^2}$; $A_{12} = \nu A_{11}$; $A_{66} = \dfrac{E_1}{2(1+\nu)}$; $D_{11} = \dfrac{E_3}{1-\nu^2}$; $D_{12} = \nu D_{11}$; $D_{66} = \dfrac{E_3}{2(1+\nu)}$;

$$(E_1, E_3) = \int_{-h/2-C}^{h/2-C} E(z)\left(1, z^2\right) dz.$$

Based on classical plate theory (CPT), equations of motion of FGP plates resting on Kerr elastic foundations can be expressed as [17, 18]:

$$\begin{aligned} &N_{x,x} + N_{xy,y} = I_0 \ddot{u}_0 - I_1 \ddot{w}_{0,x}; \quad N_{xy,x} + N_{y,y} = I_0 \ddot{v}_0 - I_1 \ddot{w}_{0,y}; \\ &M_{x,xx} + 2M_{xy,xy} + M_{y,yy} + q - \frac{k_l k_u}{k_l + k_u} w_0 + \frac{k_s k_u}{k_l + k_u} \nabla^2 w_0 \\ &= I_0 \ddot{w}_0 + I_1 \ddot{u}_{0,x} + I_1 \ddot{v}_{0,y} - I_2 \nabla^2 \ddot{w}_0. \end{aligned} \tag{9}$$

where: I_i are the mass moment of inertia $I_i = \displaystyle\int_{-h/2-C}^{h/2-C} \rho(z_{ns}) z^i \, dz$; $(i = 0,1,2)$;

Substituting Eq. (7) and (9) into Eq. (10) we obtain the system of equations in terms of displacements:

$$\begin{aligned} &A_{11} \frac{\partial^2 u_0}{\partial x^2} + A_{66} \frac{\partial^2 u_0}{\partial y^2} + (A_{12} + A_{66}) \frac{\partial^2 v_0}{\partial x \partial y} = I_0 \ddot{u}_0 - I_1 \ddot{w}_{0,x}; \\ &(A_{12} + A_{66}) \frac{\partial^2 u_0}{\partial x \partial y} + A_{66} \frac{\partial^2 v_0}{\partial x^2} + A_{11} \frac{\partial^2 v_0}{\partial y^2} = I_0 \ddot{v}_0 - I_1 \ddot{w}_{0,y}; \\ &-C_{11} \frac{\partial^4 w_0}{\partial x^4} - 2(C_{12} + 2C_{66}) \frac{\partial^4 w_0}{\partial x^2 \partial y^2} - C_{11} \frac{\partial^4 w_0}{\partial y^4} + q - \frac{k_l k_u}{k_l + k_u} w_0 \\ &+ \frac{k_s k_u}{k_l + k_u} \nabla^2 w_0 = I_0 \ddot{w}_0 + I_1 \ddot{u}_{0,x} + I_1 \ddot{v}_{0,y} - I_2 \nabla^2 \ddot{w}_0. \end{aligned} \tag{10}$$

3. Navier's solution for free vibration analysis

In the case of free vibration analysis, by setting the mechanical load to zero (q = 0). The simply supported boundary conditions based on CPT are as follows:

$$\begin{aligned} &\text{at } x = 0 \text{ and } x = a: \; v_0 = 0, w_0 = 0, N_x = 0, M_x = 0; \\ &\text{at } y = 0 \text{ and } y = b: \; u_0 = 0, w_0 = 0, N_y = 0, M_y = 0 \end{aligned} \tag{11}$$

The displacement solutions satisfying the boundary conditions (12) are chosen in the following form:

$$\begin{aligned} u_0(x,y,t) &= \sum_{m=1}^{\infty}\sum_{n=1}^{\infty} u_{0mn} e^{i\omega_{mn}t} \cos\alpha x \sin\beta y; \\ v_0(x,y,t) &= \sum_{m=1}^{\infty}\sum_{n=1}^{\infty} v_{0mn} e^{i\omega_{mn}t} \sin\alpha x \cos\beta y; \\ w_0(x,y,t) &= \sum_{m=1}^{\infty}\sum_{n=1}^{\infty} w_{0mn} e^{i\omega_{mn}t} \sin\alpha x \sin\beta y. \end{aligned} \tag{12}$$

in which:

$i = \sqrt{-1}$; $\alpha = \frac{m\pi}{a}$, $\beta = \frac{n\pi}{b}$; m, n are the number of sine half-wavelength in the x,y axes (reflect the vibration form);

$u_{0mn}, v_{0mn}, w_{0mn}$ are unknown coefficients need to be determined;

ω_{mn} is the angular natural frequency with mode (m, n), respectively.

Substituting Eq. (13) into Eq. (11), we obtain:

$$\left(\begin{bmatrix} s_{11} & s_{12} & 0 \\ s_{12} & s_{22} & 0 \\ 0 & 0 & s_{33} \end{bmatrix} - \omega_{mn}^2 \begin{bmatrix} m_{11} & 0 & m_{13} \\ 0 & m_{11} & m_{23} \\ m_{13} & m_{23} & m_{33} \end{bmatrix} \right) \begin{Bmatrix} u_{0mn} \\ v_{0mn} \\ w_{0mn} \end{Bmatrix} = \begin{Bmatrix} 0 \\ 0 \\ 0 \end{Bmatrix} \tag{13}$$

or in the form of a simple matrix form:

$$\left(\left[K_{mn}^{kc} \right] - \omega_{mn}^2 \left[M_{mn} \right] \right) \left\{ Q_{mn} \right\} = \left\{ 0 \right\} \tag{14}$$

where: $s_{11} = A_{11}\alpha^2 + A_{66}\beta^2$; $s_{12} = (A_{12} + A_{66})\alpha\beta$; $s_{22} = A_{66}\alpha^2 + A_{11}\beta^2$;

$$s_{33} = C_{11}\left(\alpha^2 + \beta^2\right)^2 + \frac{k_l k_u}{k_l + k_u} + \frac{k_s k_u}{k_l + k_u}\left(\alpha^2 + \beta^2\right)$$

$$m_{11} = I_0;\; m_{13} = -I_1\alpha;\; m_{23} = -I_1\beta;\; m_{33} = I_0 + I_2\left(\alpha^2 + \beta^2\right).$$

For each pair of values *(m, n)*, we can determine the respective natural frequency by the criterion of non-trivial displacement solution of Eq. (15).

4. Numerical results and discussion

Based on the above mentioned presented analytical solution, Matlab's code is built to implement numerical examples. The rectangular FGP plate is resting on the Keer elastic foundation, all four edges of the plates are simply supported. The porous materials made of aluminium with the physical properties are as follows: $\nu = 0.3$; $\rho_1 = 2707$ kg/m^3; $G_1 = 26{,}923$ GPa; $E_1 = 2G_1(1+\nu)$ [19]. For convenience, the non-dimensional results are used in the form [12]:

$$\varpi = \omega h\sqrt{\frac{\rho_{\max}}{E_{\max}}};\ K_l = \frac{k_l a^4}{D_m};\ K_u = \frac{k_u a^4}{D_m};\ K_s = \frac{k_s a^2}{D_m};\ D_m = \frac{E_{\max} h^3}{12\left(1-\nu^2\right)} \tag{15}$$

4.1. Validation examples

In this section, the natural frequency of simply supported square isotropic plates made of aluminum (E_m = 380 Gpa, ρ_m = 3800 kg/m^3) and alumina (E_m = 70 Gpa, ρ_m = 2702 kg/m^3); ν = 0,3 resting on Kerr's elastic foundation are validated with existing results of Shahsavari et al. [12]. The obtained results are presented in Table 1 with non-dimensional parameters computed in the form $\varpi = \omega_0 h\sqrt{\rho_m / E_m}$; $K_l = 100$; $K_u = k_u a^4 / D_m$ and four types of elastic foundation (K_u, K_s). Shahsavari and his co-workers used quasi-3D solution and first-order shear deformation theory.

Table 1. Non-dimensional fundamental frequency ϖ of isotropic square plate ($K_l = 100$, *a/h* = 20)

K_u	K_s	Source	Isotropic plate	
			Ceramic - Al_2O_3	Metal - Al
100	0	Shahsavari et al. [12]	0.0294	0.0157
		Present	**0.0296**	**0.0158**
100	100	Shahsavari et al. [12]	0.0356	0.0285
		Present	**0.0357**	**0.0285**
200	100	Shahsavari et al. [12]	0.0375	0.0317
		Present	**0.0377**	**0.0318**
200	200	Shahsavari et al. [12]	0.0440	0.0419
		Present	**0.0442**	**0.0420**

Table 2 tabulated non-dimensional natural frequencies ϖ of simply supported square FGP plate (*a/h* = 10) with various porosity coefficients. The present results are compared with those of Rezaei and Saidi [19] using the state space method, and of Thang et al. [20] using the Navier solution.
As illustrated in Table 1- 2, very good agreements between proposed model and reported studies can be clearly observed.

Table 2. Non-dimensional fundamental frequency $\varpi = \omega h\sqrt{\rho_1 / E_1}$ of porous square plate - nonuniform asymmetric (*a/h* = 10)

Source	e_0 = 0.1	e_0 = 0.3	e_0 = 0.5	e_0 = 0.7
Rezaei and Saidi [19]	0.0570	0.0551	0.0526	0.0491
Thang et al. [20]	0.0574	0.0555	0.0531	0.0495
Present	**0.0584**	**0.0565**	**0.0540**	**0.0503**

4.2. Parametric studies

The fundamental natural frequencies of simply supported rectangular FGP plates are predited with following input data: G_1 = 26,923 GPa; ρ_1 = 2702 kg/m^3; h = 0.01 m; *a/h* = 50; *b/a* = 1; $m = n = 1$.
The effect of porosity coefficient and porosity distribution patterns on fundamental natural frequencies is shown in Figure 2. It can be seen that for the FGP plate without an elastic foundation (Fig. 2a): the non-dimensional natural frequency decreases as the porosity coefficient increases for uniform porosity distribution and non-uniform asymmetric porosity distribution with the same quantitative and qualitative trend, while symmetric porosity distribution gives the opposite result.

This can be explained by the correlation between the mass effect and flexural stiffness effect of FGP plates with individual porosity distribution patterns when the porosity coefficient varies. For the FGP plate resting on the elastic foundation (Fig. 2b), the non-dimensional natural frequency increases as the porosity coefficient increases for all three porosity distribution patterns.

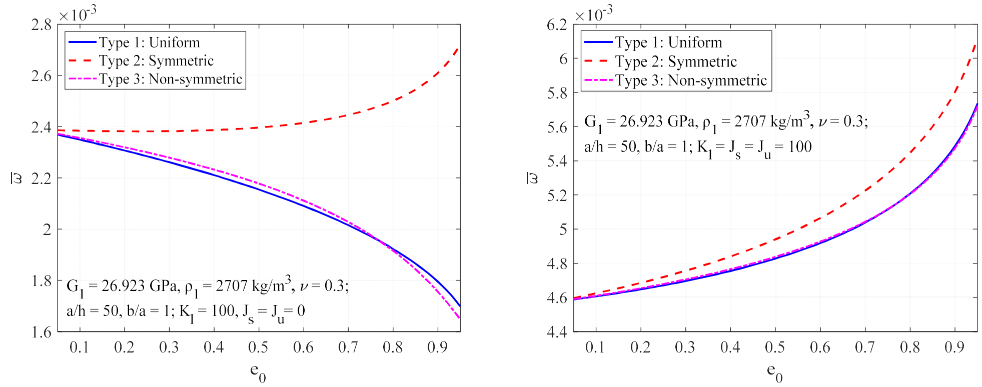

(a): Without elastic foundations (b): Rested on Kerr elastic foundations

Fig. 2. Variation of the non-dimensional natural frequency of FGP plate with porosity coefficients e_0 and various porosity distribution patterns.

Fig. 3 illustrates the effect of aspect ratio (*b/a*) and side-to-thickness ratio (*a/h*) on non-dimensional natural frequency. It is observed from the results that by increasing *b/a* and *a/h* ratios, the non-dimensional natural frequency decreases, significantly decreases in a small range of *b/a* and *a/h* ratios, and then slows down.

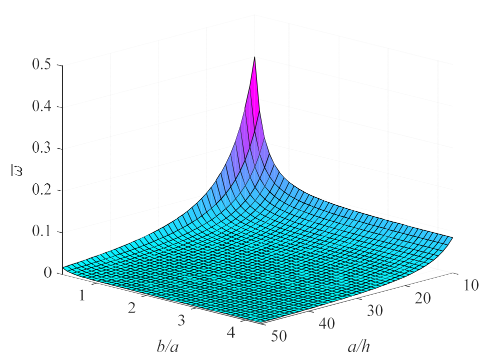

$K_u = K_s = K_l = 100$, e_0 = 0.5; Type 3;

Fig. 3. Variation of non-dimesional natural frequency of the FGP plate versus *b/a* and *a/h* ratios.

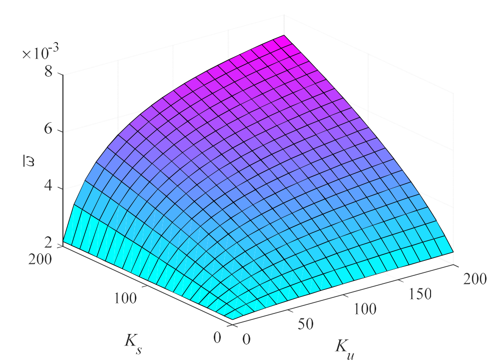

e_0 = 0.5; Type 3; *a/h* = 50, *b/a* = 1

Fig. 4. Variation of the non-dimensional natural frequency of the FGP plate versus elastic foundation stiffness.

Fig. 4 depicts the effect of elastic foundation stiffnesses on the non-dimensional natural frequency of the FGP plate. From plots can be seen that non-dimensional fundamental natural frequency increases significantly as elastic foundation stiffness (K_u, K_s) increases.

5. Conclusion

In this paper, free vibration analysis of a simply supported rectangular FGP plate resting on Kerr's elastic foundation is implemented in the framework of classical plate theory. Navier's solution has been employed to predict the natural frequency. The validation examples are carried out to confirm the accuracy of self-written Matlab code and theoretical model. The significant effect of geometrical parameters (*b/a* and *a/h* ratios), porosity distribution patterns, porosity coefficient, and elastic foundation stiffness on the natural frequency of FGP plate is indicated through various numerical examples.

References

1. Chen, D., J. Yang, and S. Kitipornchai, *Free and forced vibrations of shear deformable functionally graded porous beams*. International journal of mechanical sciences, 2016. **108**: p. 14-22.
2. Wattanasakulpong, N. and V. Ungbhakorn, *Linear and nonlinear vibration analysis of elastically restrained ends FGM beams with porosities*. Aerospace Science and Technology, 2014. **32**(1): p. 111-120.
3. Leclaire, P., K. Horoshenkov, and A. Cummings, *Transverse vibrations of a thin rectangular porous plate saturated by a fluid*. Journal of Sound and Vibration, 2001. **247**(1): p. 1-18.
4. Zhao, J., et al., *Three-dimensional exact solution for vibration analysis of thick functionally graded porous (FGP) rectangular plates with arbitrary boundary conditions*. Composites Part B: Engineering, 2018. **155**: p. 369-381.
5. Zhao, J., et al., *Free vibrations of functionally graded porous rectangular plate with uniform elastic boundary conditions*. Composites Part B: Engineering, 2019. **168**: p. 106-120.
6. Demirhan, P.A. and V. Taskin, *Bending and free vibration analysis of Levy-type porous functionally graded plate using state space approach*. Composites Part B: Engineering, 2019. **160**: p. 661-676.
7. Tran, T.T., Q.-H. Pham, and T. Nguyen-Thoi, *Static and free vibration analyses of functionally graded porous variable-thickness plates using an edge-based smoothed finite element method*. Defence Technology, 2021. **17**(3): p. 971-986.
8. Arani, A.G., et al., *Free vibration of embedded porous plate using third-order shear deformation and poroelasticity theories*. Journal of Engineering, 2017. **2017**.
9. Hashemi, S., et al., *Nonlinear free vibration analysis of In-plane Bi-directional functionally graded plate with porosities resting on elastic foundations*. International Journal of Applied Mechanics, 2022: p. 2150131.
10. Benferhat, R., et al., *Effect of porosity on the bending and free vibration response of functionally graded plates resting on Winkler-Pasternak foundations*. Earthquakes and Structures, 2016. **10**(6): p. 1429-1449.
11. Huang, X.-L., et al., *Nonlinear free and forced vibrations of porous sigmoid functionally graded plates on nonlinear elastic foundations*. Composite Structures, 2019. **228**: p. 111326.
12. Shahsavari, D., et al., *A novel quasi-3D hyperbolic theory for free vibration of FG plates with porosities resting on Winkler/Pasternak/Kerr foundation*. Aerospace Science and Technology, 2018. **72**: p. 134-149.
13. Kim, J., K.K. Żur, and J. Reddy, *Bending, free vibration, and buckling of modified couples stress-based functionally graded porous micro-plates*. Composite Structures, 2019. **209**: p. 879-888.
14. Daikh, A.A., *Temperature dependent vibration analysis of functionally graded sandwich plates resting on Winkler/Pasternak/Kerr foundation*. Materials Research Express, 2019. **6**(6): p. 065702.
15. Barati, M.R. and A.M. Zenkour, *Investigating post-buckling of geometrically imperfect metal foam nanobeams with symmetric and asymmetric porosity distributions*. Composite Structures, 2017. **182**: p. 91-98.
16. Banhart, J., *Manufacture, characterisation and application of cellular metals and metal foams*. Progress in materials science, 2001. **46**(6): p. 559-632.
17. Reddy, J.N., *Theory and analysis of elastic plates and shells*. 2006: CRC press.
18. Kneifati, M.C., *Analysis of plates on a Kerr foundation model*. Journal of Engineering Mechanics, 1985. **111**(11): p. 1325-1342.

19. Rezaei, A. and A. Saidi, *Application of Carrera Unified Formulation to study the effect of porosity on natural frequencies of thick porous–cellular plates*. Composites Part B: Engineering, 2016. **91**: p. 361-370.
20. Thang, P.T., et al., *Elastic buckling and free vibration analyses of porous-cellular plates with uniform and non-uniform porosity distributions*. Aerospace Science and Technology, 2018. **79**: p. 278-287.